A Bowl-Shaped Phosphine as a Ligand in Rhodium-Catalyzed Hydrosilylation: Rate Enhancement by a Mono(phosphine) Rhodium Species

Osamu Niyomura,[†] Tetsuo Iwasawa, Naoki Sawada, Makoto Tokunaga,
Yasushi Obora, and Yasushi Tsuji*

*Catalysis Research Center and Division of Chemistry, Graduate School of Science,
Hokkaido University, CREST, Japan Science and Technology Corporation (JST),
Sapporo 001-0021, Japan*

Bowl-shaped phosphine (BSP) ligands markedly accelerated the rhodium-catalyzed hydrosilylation of ketones and ketimines as compared with the effect of conventional phosphine ligands such as PPh$_3$ and P(*t*-Bu)$_3$. ^{31}P NMR study of a mixture of [RhCl(C$_2$H$_4$)$_2$]$_2$ and phosphines at various P/Rh ratios revealed that coordination of BSP to the rhodium metal was successfully regulated, and the resultant rhodium complex bearing only one phosphine ligand (a mono(phosphine) rhodium species) was responsible for the acceleration. Structural comparison between BSP and the conventional phosphines was carried out using HF/6-31G(d)-CONFLEX/MM3-optimized structures. The mono(phosphine) rhodium complex having 1,5-cyclooctadiene as a ligand was isolated, and its X-ray molecular structure was determined.

Introduction

Phosphines are one of the most important ligands in a homogeneous transition-metal-catalyzed reaction.[1] Therefore, a wide variety of phosphines have been designed and synthesized to realize highly active and selective catalytic reactions. As a ligand, the steric (bulkiness) and electronic effects (basicity) of phosphines are particularly important. Recently, very bulky and basic phosphines such as P(*t*-Bu)$_3$ and tricyclohexyl-phosphine (PCy$_3$) were found to be effective ligands in several transition-metal-catalyzed reactions.[2] On the other hand, as a new class of phosphines, the first bowl-shaped[3] phosphine (BSP), tris(2,2″,6,6″-tetramethyl-*m*-terphenyl-5′-yl)phosphine (**1**; Figure 1A), was recently synthesized.[4] Parts A and E of Figure 2 show structures of **1** and P(*t*-Bu)$_3$ which were optimized by ab initio HF/

† Present address: Division of Chemistry, College of Liberal Arts and Sciences, Kitasato University.
(1) (a) *Homogeneous Catalysis with Metal Phosphine Complexes*; Pignolet, L. H., Ed.; Plenum: New York, 1983. (b) Brandsma, L.; Vasilevsky, S. F.; Verkruijsse, H. D. *Applications of Transition Metal Catalysts in Organic Synthesis*; Springer: Berlin, 1999.
(2) (a) Littke, A. F.; Dai, C.; Fu, G. C. *J. Am. Chem. Soc.* **2000**, *122*, 4020−4028. (b) Kirchhoff, J. H.; Dai, C.; Fu, G. C. *Angew. Chem., Int. Ed.* **2002**, *41*, 1945−1947. (c) Littke, A. F.; Fu, G. C. *Angew. Chem., Int. Ed.* **2002**, *41*, 4176−4211. (d) Kataoka, N.; Shelby, Q.; Stambuli, J. P.; Hartwig, J. F. *J. Org. Chem.* **2002**, *67*, 5553−5556. (e) Walker, S. D.; Barder, T. E.; Martinelli, J. R.; Buchwald, S. L. *Angew. Chem., Int. Ed.* **2004**, *43*, 1871−1876.
(3) (a) Maverick, E.; Cram, D. J. In *Comprehensive Supramolecular Chemistry*; Vögtle, F., Ed.; Elsevier: Oxford, U.K., 1996; Vol. 2, pp 367−418. (b) Goto, K.; Okumura, T.; Kawashima, T. *Chem. Lett.* **2001**, 1258−1259. (c) Goto, K.; Nagahama, M.; Mizushima, T.; Shimada, K.; Kawashima, T.; Okazaki, R. *Org. Lett.* **2001**, *3*, 3569−3572. (d) Naiki, M.; Shirakawa, S.; Kon-i, K.; Kondo, Y.; Maruoka, K. *Tetrahedron Lett.* **2001**, 42, 5467−5471. (e) Ohzu, Y.; Goto, K.; Kawashima, T. *Angew. Chem., Int. Ed.* **2003**, *42*, 5714−5717.
(4) (a) Goto, K.; Ohzu, Y.; Sato, H.; Kawashima, T. *Abstr. Pap. 15th Int. Conf. Of Phosphorous Chemistry (Sendai, Japan)* **2001**, 236. (b) Goto, K.; Ohzu, Y.; Sato, H.; Kawashima, T. *Phosphorus, Sulfur, Silicon Relat. Elem.* **2002**, *177*, 2179.
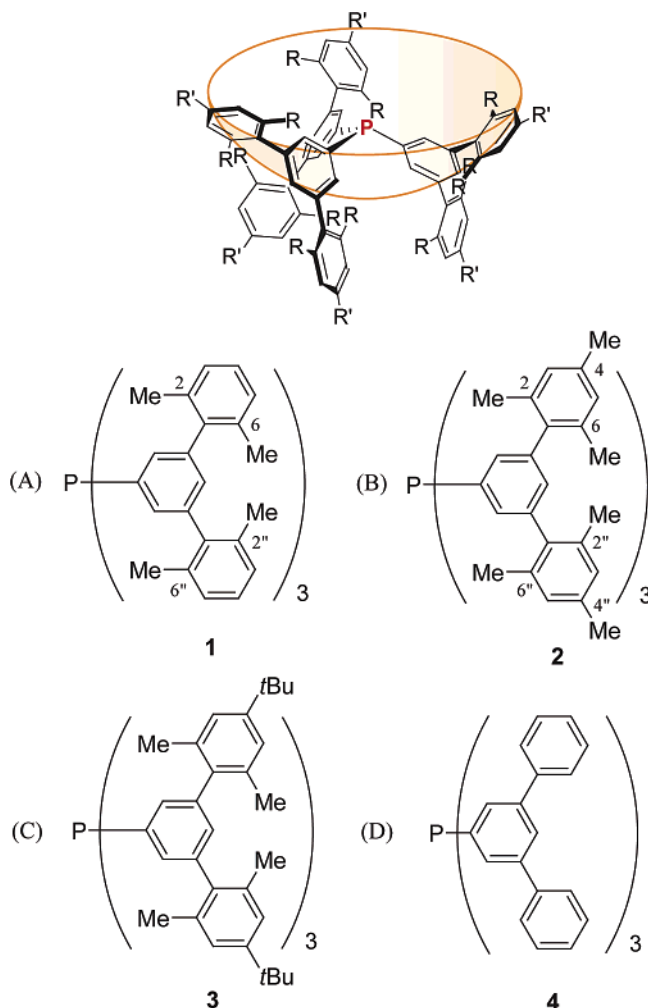

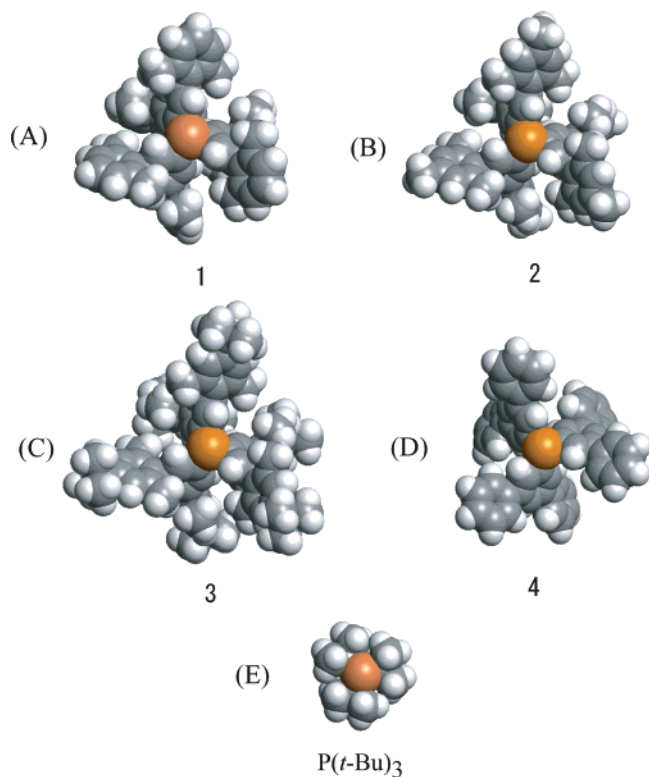**Figure 1.** Bowl-shaped phosphines.

Figure 2. Optimized structures (top view) of **1**−**4** and P(*t*-Bu)$_3$.

6-31G(d) calculations[5] using initial structures optimized by CONFLEX[6a]/MM3.[6b,c] As shown in Figure 2A,E, both **1** and P(*t*-Bu)$_3$ are obviously very bulky. However, the nature of the bulkiness is quite different between these two phosphines. The bulkiness of the bowl-shaped phosphine (**1**) occurs on the periphery of the phosphine (at the rim of the bowl) with substantial empty space around the phosphorus atom.[7] In contrast, P(*t*-Bu)$_3$ has severe steric congestion within close proximity of the phosphorus atom. Owing to this notable feature, BSP ligands may bring about a unique catalytic environment in homogeneous transition-metal catalysis, which cannot be realized with conventional phosphines.

With BSP as a ligand, we started a transition-metal-catalyzed reaction, since there were no precedents for

(5) Frisch, M. J.; Trucks, G. W.; Schlegel, H. B.; Scuseria, G. E.; Robb, M. A.; Cheeseman, J. R.; Zakrzewski, V. G.; Montgomery, J. A., Jr.; Stratmann, R. E.; Burant, J. C.; Dapprich, S.; Millam, J. M.; Daniels, A. D.; Kudin, K. N.; Strain, M. C.; Farkas, O.; Tomasi, J.; Barone, V.; Cossi, M.; Cammi, R.; Mennucci, B.; Pomelli, C.; Adamo, C.; Clifford, S.; Ochterski, J.; Petersson, G. A.; Ayala, P. Y.; Cui, Q.; Morokuma, K.; Malick, D. K.; Rabuck, A. D.; Raghavachari, K.; Foresman, J. B.; Cioslowski, J.; Ortiz, J. V.; Stefanov, B. B.; Liu, G.; Liashenko, A.; Piskorz, P.; Komaromi, I.; Gomperts, R.; Martin, R. L.; Fox, D. J.; Keith, T.; Al-Laham, M. A.; Peng, C. Y.; Nanayakkara, A.; Gonzalez, C.; Challacombe, M.; Gill, P. M. W.; Johnson, B. G.; Chen, W.; Wong, M. W.; Andres, J. L.; Head-Gordon, M.; Replogle, E. S.; Pople, J. A. *Gaussian 98*, revision A.7; Gaussian, Inc.: Pittsburgh, PA, 1998.

(6) (a) Goto, H. *J. Am. Chem. Soc.* **1989**, *111*, 8950−8951. (b) Lii, J.-H. Allinger, N. L. *J. Am. Chem. Soc.* **1989**, *111*, 8566−8575. (c) Lii, J.-H. Allinger, N. L. *J. Am. Chem. Soc.* **1989**, *111*, 8576−8582.

(7) Recently we prepared pyridine ligands bearing a 2,3,4,5-tetraphenylphenyl moiety at the 3-position. The pyridine ligands have steric congestion at remote positions from the coordination center (nitrogen). This "long-range steric effect" of the pyridine ligands successfully suppresses Pd black formation in air oxidation of alcohols: Iwasawa, T.; Tokunaga, M.; Obora, Y.; Tsuji, Y. *J. Am. Chem. Soc.* **2004**, *126*, 6554−6555.

Table 1. Rhodium-Catalyzed Hydrosilylation of Cyclohexanone with Various Ligands[a]

entry	ligand	P/Rh	yield, %[b]
1	**1**	1	76
2	**1**	2	97
3	**1**	3	85
4	**2**	2	93
5	**3**		92
6	**4**	1	30
7	**4**	2	40
8	**4**	3	<1
9	PPh$_3$	1	27
10		2	9
11		3	<1
12	P(2-furyl)$_3$	2	22
13	P(*o*-tol)$_3$		32
14	PMes$_3$		25
15	PEt$_3$		<2
16	P(*t*-Bu)$_3$		31
17	PCy$_3$		<2

[a] Conditions: cyclohexanone (1 mmol), silane (1.2 mmol), [RhCl(C$_2$H$_4$)$_2$]$_2$ (5.0 μmol), ligand (0.01−0.03 mmol), benzene (1 mL), at room temperature for 3 h. [b] Determined by GC.

catalytic reactions with BSP as a ligand.[8] In this paper, we carried out the rhodium-catalyzed hydrosilylation[9] with BSP as a ligand and found remarkable rate enhancement[10] owing to a mono(phosphine) rhodium species. Here, we describe a full detail and reaction mechanism for the rate enhancement.

Results

Several BSP species were synthesized. They are tris-(*m*-terphenyl)phosphine derivatives having substituents at the 2,2″,6,6″- (**1**) and 2,2″,4,4″,6,6″-positions (**2**, **3**), along with a derivative without substituents at these positions (**4**) (Figure 1). They were synthesized straightforwardly by lithiation of the corresponding *m*-terphenyl bromides followed by a reaction with PCl$_3$. The structures of **1**−**4** were optimized by HF/6-31G(d)-CONFLEX/MM3 calculations, as shown in Figure 2A−D, which shows that all of the phosphines **1**−**4** have bowl-shaped structures with the phosphorus atom at the bottom of the bowl.

Hydrosilylation of Ketones and Ketimines. To examine the efficacy of a BSP as a ligand, the rhodium-catalyzed hydrosilylation of cyclohexanone with HSiMe$_2$-Ph as the silane was carried out. The bowl-shaped phosphines **1**−**4** and other conventional phosphines were employed as the ligand at a P/Rh ratio of 2 in the presence of 0.5 mol % [RhCl(C$_2$H$_4$)$_2$]$_2$ (Table 1). The reactions were carried out at room temperature for 3 h, and yields of the products at that time were determined after desilylation. The use of **1**, bearing methyl substituents at the 2,2″,6,6″-positions, gave cyclohexanol in

(8) Palladium complexes bearing the bowl-shaped phosphines were reported: (a) Matsumoto, T.; Kasai, T. Tatsumi, K. *Chem. Lett.* **2002**, 346−347. (b) Ohzu, Y.; Goto, K.; Kawashima, T. *Angew. Chem., Int. Ed.* **2003**, *42*, 5714−5717.

(9) Ojima, I. In *The Chemistry of Organic Silicon Compounds*; Patai, S., Rappoport, Z., Eds.; Wiley: Chichester, U.K., 1989; Chapter 25.

(10) A portion of this work was preliminarily reported: Niyomura, O.; Tokunaga, M.; Obora, Y.; Iwasawa, T.; Tsuji, Y. *Angew. Chem., Int. Ed.* **2003**, *42*, 1287−1289.

97% yield (entry 2). Similarly, **2** and **3** having methyl and/or *tert*-butyl groups at the 2,2″,4,4″,6,6″-positions also afforded the product at P/Rh = 2 in 93% and 92% yields, respectively (entries 4 and 5). However, the phosphine without the substituents at these positions (**4**) was not efficient in affording the product, giving 40% yield after 3 h (entry 7). It is noteworthy that these structurally comparable ligands (**1−3** and **4**) show different efficiencies in the reaction. The methyl substituents at the 2,2″,6,6″-positions of **1−3** apparently play a critical role in realizing the high catalytic activity, even though these methyl substituents are rather distant from the phosphorus atoms of **1−3**.

The ligands **1−4** are classified as triarylphosphines. Therefore, several conventional triarylphosphines were employed in the reaction for comparison. As a result, PPh$_3$ and P(2-furyl)$_3$[11] at P/Rh = 2 afforded the products in only 9% and 22% yields, respectively (entries 10 and 12). Furthermore, the typical bulky triarylphosphines P(*o*-tolyl)$_3$[11] and P(Mes)$_3$[11] afforded the product in 32% and 25% yields, respectively (entries 13 and 14). Use of the basic trialkylphosphine PEt$_3$ as the ligand provided the product in <2% yield (entry 15), and representative bulky basic trialkylphosphines such as P(*t*-Bu)$_3$ and PCy$_3$ were also less effective and resulted in 31% and <2% yields, respectively (entries 16 and 17). Thus, these results clearly indicated that **1−3**, bearing methyl substituents at the 2,2″,6,6″-positions, specifically enhance the catalytic activity.

In the reaction, the P/Rh ratio has a significant effect on the catalytic activity (Table 1). When **1** was employed as the ligand, the ratio P/Rh = 1−3 did not change the yields substantially (entries 1−3). In contrast, with **4** and PPh$_3$ as the ligands, the ratio affected the yield considerably (entries 6−8 and entries 9−11). The most evident difference was observed at P/Rh = 3: for this ratio, the catalyst system with **1** was still active in affording the product in 85% yield (entry 3), whereas with **4** and PPh$_3$ almost no catalytic activity was observed (entries 8 and 11). In this way, even though excess **1** did not affect the catalytic activity, excess **4** and PPh$_3$ deactivated the catalyst significantly.

Even the reactions with **4** and the conventional ligands were very sluggish at P/Rh = 2 (entries 7, 10, and 12−17); these catalysts were still living for a long time, and the product was obtained in good yields (>70%) with a much longer reaction time (40−500 h). Accordingly, the diverse yields in Table 1 were caused by different reaction rates of the hydrosilylation. Thus, a kinetic study was carried out at 24 °C with **1**, **4**, PPh$_3$, and P(*o*-tol)$_3$ as the representative ligands under the same reaction conditions as in Table 1. The reaction rates with these triarylphosphines showed a first-order dependence on both the ketone and silane concentrations: rate = k_{obs}[ketone][silane]. The observed rate constants (k_{obs}) with **1**, **4**, PPh$_3$, and P(*o*-tol)$_3$ were 4.79 ± 0.36, 0.154 ± 0.004, 0.0031 ± 0.0013, and 0.169 ± 0.003 mol^{-1} dm^3 h^{-1}, respectively. The results indicated that the catalyst system with **1** realized a remarkable rate enhancement, in which reactions that were 154, 31, and 28 times faster as compared with those with PPh$_3$, **4**, and P(*o*-tol)$_3$, respectively, were observed.

(11) P(2-furyl)$_3$, P(*o*-tolyl)$_3$, and P(Mes)$_3$ denote tri-2-furylphosphine, tri-*o*-tolylphosphine, and tris(2,4,6-trimethylphenyl)phosphine, respectively.

Table 2. Hydrosilylation of Ketones and Ketimines[a,b]

entry	substrate	silane	ligand	P/Rh	t(h)	%yield[c]
1	cyclohexanone	HSiEt$_3$	**1**	2	21	81
2			**4**			36
3			PPh$_3$			13
4	cyclohexanone	HSiMePh$_2$	**1**	2	20	97
5			**4**			37
6			PPh$_3$			27
7	acetophenone	HSiMe$_2$Ph	**1**	2	5	96
8			**4**			15
9			PPh$_3$			15
10[d]	2-octanone	HSiMe$_2$Ph	**1**	2	6	91
11[d]			**4**			41
12[d]			PPh$_3$			31
13	(-)-menthone	HSiMe$_2$Ph	**1**	2	20	92 (45/55)[e]
14			**4**			8 (43/57)[e]
15			PPh$_3$			12 (38/62)[e]
16[f]	cyclohexanone	HSiMe$_2$Ph	**1**	2	6	95
17[f]			**4**			65
18[f]			PPh$_3$			9
19	Ph, Ph >=N, Ph Ph	HSiMe$_2$Ph	**1**	1	16	18
20				2		88
21				4		93
22			**4**	1	16	3
23				2		6
24				4		<1
25			PPh$_3$	1	16	16
26				2		24
27				4		6
28[g]	Me, Ph >=N, Ph Ph	HSiMe$_2$Ph	**1**	2	8	80
29[g]			**4**			12
30[g]			PPh$_3$			13
31[h]	⬡=N, Ph	HSiMe$_2$Ph	**1**	2	8	88
32[h]			**4**			<1
33[h]			PPh$_3$			5

[a] Conditions: ketone (1 mmol), silane (1.2 mmol), [RhCl(C$_2$H$_4$)$_2$]$_2$ (5 μmol), ligand (20 μmol), in benzene (1 mL) at room temperature. [b] Conditions: imine (0.25 mmol), silane (0.60 mmol), [RhCl(C$_2$H$_4$)$_2$]$_2$ (3.75 μmol), ligand, in toluene (0.5 mL) at 60 °C. [c] Yield of alcohol and amine by GC after the desilylation with HCl/MeOH. [d] At 50 °C. [e] Product ratio (neomenthol/menthol). [f] [Rh(COD)$_2$]BF$_4$ (10 μmol) was used instead of [RhCl(C$_2$H$_4$)$_2$]$_2$ in CH$_2$Cl$_2$ as solvent. [g] [RhCl(C$_2$H$_4$)$_2$]$_2$ (2.5 μmol). [h] Conditions: imine (1 mmol), silane (1.2 mmol), [RhCl(C$_2$H$_4$)$_2$]$_2$ (5 μmol), ligand (20 μmol), in toluene (1 mL) at 40 °C.

The rate enhancement was further confirmed in the hydrosilylation of various silanes and ketones (Table 2). As the silane, like HSiMe$_2$Ph in Table 1, HSiEt$_3$ afforded cyclohexanol in much higher yield (81%) with **1** (entry 1) than with **4** (36% yield, entry 2) and PPh$_3$ (13% yield, entry 3). With HSiMePh$_2$, **1** also provided the product in higher yield (97%) than with **4** (37% yield) and PPh$_3$ (27% yield) (entries 4−6). Furthermore, the distinct rate enhancement with **1** as compared with **4** and PPh$_3$ was also observed in the hydrosilylation of various ketones such as acetophenone (yields of the product: 96% with **1**, 15% with **4**, 15% with PPh$_3$, entries 7−9), 2-octanone (yields of the product: 91% with **1**, 41% with **4**, 31% with PPh$_3$, entries 10−12), and (−)-menthone (yields of the product: 92% with **1**, 8% with **4**, 12% with PPh$_3$, entries 13−15). As the catalyst precursor, the cationic rhodium complex [Rh(COD)$_2$]BF$_4$ (COD = 1,5-cyclo-octadiene) also showed a rate enhancement with **1** (entries 16−18).

Table 3. Hydrosilylation of 2-Methylbenzaldehyde[a]
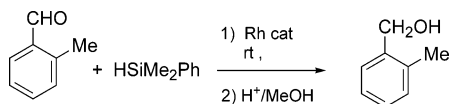
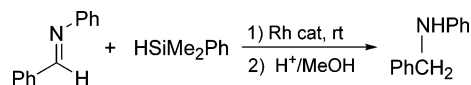| entry	P/Rh	ligand	yield, %[b]
1	2	**1**	90
2		**4**	90
3		PPh₃	82
4	4	**1**	50
5		**4**	40
6		PPh₃	7

[a] Conditions: aldehyde (1 mmol), silane (1.2 mmol), [RhCl-(C₂H₄)₂]₂ (5 µmol), ligand (20 or 40 µmol), benzene (1 mL) at room temperature for 6 h. [b] Yield of alcohol by GC after desilylation with HCl/MeOH.

Since the hydrosilylation of ketones is exceedingly accelerated with **1** as the ligand, the hydrosilylation of ketimines was also examined with **1**, **4**, and PPh₃ as the ligands (Table 2, entries 19−33). In the hydrosilylation of benzophenone-*N*-phenylimine with **1** as the ligand, the corresponding amine was obtained in 88% yield at P/Rh = 2 after the desilylation (entry 20). Similar to the hydrosilylation of ketones (Table 1 and entries 1−18 in Table 2), **4** and PPh₃ afforded the hydrosilylated product in only low yields, 6% and 24%, respectively, at P/Rh = 2 (entries 23 and 26). Moreover, in the hydrosilylation of acetophenone-*N*-phenylimine (entries 28−30) and cyclohexanone-*N*-phenylimine (entries 31−33), **1** was also a far more efficient ligand than **4** and PPh₃. Notably, as observed with ketones (Table 1), excess **1** did not affect the catalytic activity (entries 21), while excess **4** and PPh₃ suppressed the catalyst activity considerably (entries 24 and 27).

Hydrosilylation of Aldehydes, Aldimines, and Alkenes. Furthermore, hydrosilylation of aldehydes was attempted. The representative results with 2-methylbenzaldehyde are shown in Table 3. At the ratio of P/Rh = 2, the yields with **1**, **4**, and PPh₃ were high: 90%, 90%, and 82%, respectively (entries 1−3). At P/Rh = 4, however, the yield with PPh₃ was reduced to 7% (entry 6), while the yields with **1** and **4** were still moderate (entries 4 and 5). Other various aldehydes showed more or less similar behavior in the reaction. Thus, the ligands somehow influence the hydrosilylation of aldehydes, but the distinct rate enhancement with **1** such as observed with ketones and ketimines was not evident.

With respect to aldimine as the substrate, the hydrosilylation of benzaldehyde-*N*-phenylimine was carried out (Table 4). At P/Rh = 2, **1** and PPh₃ afforded the corresponding amine in high yields after the desilylation (entries 1 and 3), but **4** did not provide the product (entry 2). With excess ligand (P/Rh = 4), **1** did not suppress the reaction (entry 4), but almost no catalytic activity was observed with excess **4** and PPh₃ (entries 5 and 6).

Finally, the hydrosilylation of 1-hexene was carried out (Table 5). At P/Rh = 2, no particular rate enhancement associated with **1** was evident (entries 1−3). However, again, with excess ligand at P/Rh = 4, no catalytic activity appeared with **4** and PPh₃, while excess **1** did not affect the catalytic reaction.

Table 4. Hydrosilylation of Benzaldehyde-*N*-phenylimine[a]

entry	P/Rh	ligand	yield, %[b]
1	2	**1**	79
2		**4**	0
3		PPh₃	78
4	4	**1**	85
5		**4**	0
6		PPh₃	<1

[a] Conditions: imine (2.5 mmol), silane (3.0 mmol), [RhCl(C₂H₃)₂]₂ (2.5 µmol), ligand (10 or 20 µmol), at room temperature for 8 h. [b] Yield of amine by GC after desilylation with HCl/MeOH.

Table 5. Hydrosilylation of 1-Hexene[a]
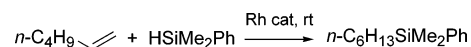
entry	P/Rh	ligand	yield, %[b]
1	2	**1**	93
2		**4**	70
3		PPh₃	87
4	4	**1**	86
5		**4**	0
6		PPh₃	3

[a] Conditions: 1-hexene (1 mmol), silane (1.2 mmol), [RhCl-(C₂H₄)₂]₂ (5 µmol), ligand (20 or 40 µmol), toluene (1 mL) at room temperature for 1 h. [b] By GC.

In this manner, in the hydrosilylation of aldehydes, aldimines, and 1-hexene, evident rate enhancement with **1** was not observed. However, in these reactions, the behavior of excess ligand is quite different. Especially, in the hydrosilylation of the aldimine (Table 4) and 1-hexene (Table 5), excess **1** did not suppress the catalyst activity at all, while excess **4** and PPh₃ almost inhibit the catalytic activity.

Discussion

The BSP ligands **1**−**3** gave distinct rate enhancements in the hydrosilylation of ketones and ketimines. However, the structurally comparable **4** and the conventional ligands listed in Table 1 are not effective.

Basicity and Cone Angle. To elucidate the rationale for the ligands (**1**−**3**) to enhance the catalytic activity, two critical parameters, basicity and cone angle, were examined. In this study, the basicity of the phosphines was evaluated by two established methods. One is theoretical calculation (HF/6-31G(d) level) of the molecular electrostatic potential minimum (V_{min}) according to the method of Koga et al.:[12] more negative V_{min} values indicate more basic phosphines. The other is $^1J_{P-Se}$ coupling constants of the corresponding phosphine selenides Se=PR₃, which are convenient, but less reliable, measures of the basicity of the parent phosphines PR₃: smaller coupling constants correspond to higher basicities.[13] These two values are listed in Table 6. For the steric effect, the cone angle is often employed as a

(12) Suresh, C. H.; Koga, N. *Inorg. Chem.* **2002**, *41*, 1573−1578.
(13) (a) Allen, D. W.; Taylor, B. F. *J. Chem. Soc., Dalton Trans.* **1982**, 51−54. (b) Socol, S. M.; Verkade, G. J. *Inorg. Chem.* **1984**, *23*, 3487−3493. (c) Keay, B. A.; Andersen, N. G. *Chem. Rev.* **2001**, *101*, 997−1030. (d) Alyea, E. C.; Malito, J. *Phosphorus, Sulfur, and Silicon Relat. Elem.* **1989**, *46*, 175−181.

Table 6. Basicities and Cone Angles of the Phosphines

		basicity		cone angle, deg	hydrosilylation yield. %[d]
entry	ligand	V_{min}	$^1J_{P-Se}$, Hz		
1	**1**	−41.0	770	205	97
2	**2**	−42.8	741	210	93
3	**3**	−42.5	743	223	92
4	**4**	−41.6	766	193	40
5	PPh$_3$	−42.2	735[a]	168	27
6	P(2-furyl)$_3$	−38.5	793[b]	152	22
7	P(o-tol)$_3$	−44.4	732	218	32
8	PMes$_3$	−44.6	-[c]	243	25
9	PEt$_3$	−49.8	705[a]	166	<2
10	PCy$_3$	−54.4	674	188	<2
11	P(t-Bu)$_3$	−54.4	686	181	31

[a] Data in ref 13a. [b] Data in ref 13b. [c] Trimesitylphosphine selenide is not available.[13d] [d] Yields of the hydrosilylation of cyclohexanone in Table 1.

good criterion. Originally, however, Tolman measured them on "folded-back" (most-packed) CPK molecular models to minimize arbitrariness.[14] Consequently, they are appreciably smaller than those of the real phosphines. In the present study, for more accurate discussion, we measured the cone angles according to Tolman's definition using structures optimized by HF/6-31G(d)-CONFLEX/MM3 calculations (Table 6).

The basicity and/or the cone angle have so far successfully rationalized the influence of monodentate phosphines in a wide variety of homogeneous catalysis. However, in the present study, the effective (**1**−**3**, entries 1−3 in Table 6) and ineffective (**4**, entry 4) BSP ligands have essentially similar basicities comparable to that of PPh$_3$ (entry 5). They are within the range expected for the conventional triarylphosphines (entries 5−8), which did not accelerate the hydrosilylation of ketones at all (Table 1). Therefore, a simple explanation with basicity is not operative. As for the steric effect, the cone angles of the effective (**1**) and ineffective ligands (**4**) are comparable. Furthermore, a particular range of the cone angles for the effective ligands cannot be determined. Thus, neither the basicity nor the cone angles listed in Table 6 showed evident correlations with the aforementioned efficacy of the ligands.
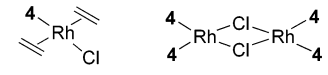
^{31}P NMR Study on a Mixture of [RhCl(C$_2$H$_4$)$_2$]$_2$ and 1 or 4. Since the excess ligands affect the catalytic reaction in a different way, as observed in Tables 1−5, the coordination behavior of the phosphines toward the catalyst precursor, [RhCl(C$_2$H$_4$)$_2$]$_2$, was examined. ^{31}P NMR spectra are most diagnostic of the coordination, since a phosphine on a Rh (^{103}Rh, $I = ^1/_2$, 100%)[15] shows informative $^1J_{P-Rh}$ coupling and the ^{31}P resonance can be unambiguously assigned according to the corresponding PPh$_3$ complexes reported in the literature.[16] The ^{31}P resonances of the Rh complexes bearing **1** or **4** are compared with the corresponding PPh$_3$ complexes in Table 7. At first, **1** and [RhCl(C$_2$H$_4$)$_2$]$_2$ were mixed at various P/Rh ratios for 2 h at room temperature, and ^{31}P NMR spectra of the mixture were measured. The

(14) Tolman, C. A. *Chem. Rev.* **1977**, 77, 313−348.
(15) Brevard, C.; Granger, P. *Handbook of High-Resolution Multinuclear NMR*; Wiley-Interscience: New York, 1981; p 158.
(16) (a) Naaktgeboren, A. J.; Nolte, R. J. M.; Drenth, W. *J. Am. Chem. Soc.* **1980**, 102, 3350−3354. (b) Elsevier, C. J.; Kowall, B.; Kragten, H. *Inorg. Chem.* **1995**, 34, 4836−4839. (c) Brown, T. H.; Green, P. J. *J. Am. Chem. Soc.* **1970**, 92, 2359−2362.

Table 7. ^{31}P Resonances of Rh Complexes Bearing 1 or 4 as the Ligand[a]

entry	complex, ^{31}P resonance	corresponding PPh$_3$ complex, ^{31}P resonance
1	*trans*-RhCl(C$_2$H$_4$)$_2$(**1**) 53.0 (d, $^1J_{P-Rh}$ = 186)	*trans*-RhCl(C$_2$H$_4$)$_2$(PPh$_3$) 53.3 (d, $^1J_{P-Rh}$ = 184)[16a]
2	*trans*-RhCl(C$_2$H$_4$)(**1**)$_2$ 33.5 (d, $^1J_{P-Rh}$ = 130)	*trans*-RhCl(C$_2$H$_4$)(PPh$_3$)$_2$ 35.4 (d, $^1J_{P-Rh}$ = 129)[16a]
3	*trans*-RhCl(C$_2$H$_4$)$_2$(**4**) 57.2 (d, $^1J_{P-Rh}$ = 187)	see entry 1
4	[RhCl(**4**)$_2$]$_2$ 56.9 (dd, J = 191, 51) 61.0 (dd, J = 193, 51)	[RhCl(PPh$_3$)$_2$]$_2$ 51.9 (d, $^1J_{P-Rh}$ = 193)[16a]
5	RhCl(COD)(**1**) 30.5 (d, $^1J_{P-Rh}$ = 153)	RhCl(COD)(PPh$_3$) 31.4 (d, $^1J_{P-Rh}$ = 152)[16b]
6	RhCl(COD)(**4**) 34.2 (d, $^1J_{P-Rh}$ = 153)	see entry 5
7	RhCl(**4**)$_3$ 39.5 (dd, J = 140, 39) 54.9 (dt, J = 186, 39)	RhCl(PPh$_3$)$_3$ 31.5 (dd, J = 142, 38)[16c] 48.0 (dt, J = 189, 38)

[a] In benzene-d_6 at room temperature; resonances given in ppm and J values given in Hz.

Scheme 1. ^{31}P NMR Study on a Mixture of [RhCl(C$_2$H$_4$)$_2$]$_2$ and the Bowl-Shaped Phosphines (*P*)

results are shown in Scheme 1A. With P/Rh = 1, only the mono(phosphine) rhodium complex *trans*-RhCl-(C$_2$H$_4$)$_2$(**1**) formed, whose ^{31}P resonance is in excellent agreement with that of the corresponding PPh$_3$ complex[16a] (Table 7, entry 1). At P/Rh = 2, still the mono-(phosphine) rhodium complex was the predominant (90% among rhodium−phosphine complexes) species with only a small amount of the bis(phosphine) rhodium complex, *trans*-RhCl(C$_2$H$_4$)(**1**)$_2$, which also coincides with the ^{31}P resonance of the corresponding PPh$_3$ complex[16a] (Table 7, entry 2). Surprisingly, even at P/Rh = 3, the mono(phosphine) complex remained dominant (90%) with a greater amount of free (uncoordinated) **1** at −8.4 ppm. Here, no tris(phosphine) complex formed at all. Thus, with **1**, over the range of P/Rh = 1−3, the mono(phosphine) rhodium complex was the prevailing (>90%) species (Scheme 1A).
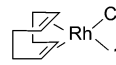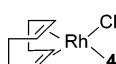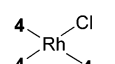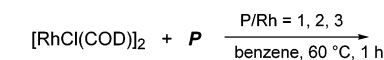
On the other hand, with **4** as BSP, the same ^{31}P NMR measurement was carried out (Scheme 1B). In contrast, the coordination behavior of **4** was quite different from that of **1**. At P/Rh = 1, a much smaller amount (17%) of the mono(phosphine) rhodium complex *trans*-RhCl-(C$_2$H$_4$)$_2$(**4**) (Table 7, entry 3) formed, and the bis-

Scheme 2. [31]**P NMR Study on a Mixture of [RhCl(COD)]₂ and the Bowl-Shaped Phosphines (*P*)**

$$[RhCl(COD)]_2 \ + \ \boldsymbol{P} \ \xrightarrow[\text{benzene, 60 °C, 1 h}]{\text{P/Rh = 1, 2, 3}}$$

(A)

	relative ^{31}P intensity	
P = 1 P/Rh =	(Rh–Cl structure) **1**	free **1**
1	> 99	~0
2	49	51
3	32	68

(B)

	relative ^{31}P intensity (mol% among Rh-*P* complexes)		
P = 4 P/Rh =	(Rh–Cl structure) **4**	**4**–Rh–Cl–**4**	free **4**
1	>99	~0	~0
2	41 (77)	36 (23)	23
3	19 (53)	50 (47)	31

(phosphine) rhodium complex [RhCl(**4**)₂]₂ was the main species (83% as a mononuclear rhodium complex). [31]P resonances of [RhCl(**4**)₂]₂ appeared as two inequivalent resonances, possibly due to a distortion caused by the large steric size of **4**, while the corresponding PPh₃ complex showed equivalent ^{31}P resonances (Table 7, entry 4). However, the formation of [RhCl(**4**)₂]₂ was unambiguously identified by an FD mass spectrum of the reaction mixture (*m/z* 3152, M⁺, 100%; *m/z* 1576, M²⁺, 7%: see the Supporting Information). At P/Rh = 3, only the bis(phosphine) rhodium complex was afforded, along with a considerable amount of free **4** (33%). As for PPh₃, the reaction with [RhCl(C₂H₄)₂]₂ afforded a considerable amount of the tris(phosphine) complex, [RhCl(PPh₃)₃],[16c] even at P/Rh = 2. Thus, the ^{31}P NMR measurements at the different P/Rh ratios revealed that the coordination behaviors of **1**, **4**, and PPh₃ toward the catalyst precursor [RhCl(C₂H₄)₂]₂ were quite different. Using **1** as the ligand, the mono(phosphine) rhodium species was predominant even at P/Rh = 3.

The BSP ligand **1** realized a far better catalytic activity in the hydrosilylation of ketones and ketimines as compared with that of **4** and PPh₃ (Table 2). Furthermore, unlike **4** and PPh₃, **1** did not lower the catalytic activity even at high P/Rh ratios (Tables 3 and 4). Thus, the mono(phosphine) complex RhCl(C₂H₄)₂ (**1**) might be responsible for the high catalytic activity. Therefore, isolation of the mono(phosphine) ethylene complex was attempted. However, all the trials to isolate RhCl(C₂H₄)₂(**1**) were unsuccessful, since the ethylene ligand is highly labile. Accordingly, we employed [RhCl-(COD)]₂ (COD = 1,5-cyclooctadiene) in place of [RhCl-(C₂H₄)]₂ in the reaction with **1** to isolate a mono-(phosphine) COD complex.

Isolation of the Mono(phosphine) Complex RhCl-(COD)(1). As shown in Scheme 2A, the similar reaction of [RhCl(COD)]₂ with **1** at P/Rh = 1 in benzene-*d*₆ at 60 °C for 1 h afforded the mono(phosphine) complex RhCl-(COD)(**1**), as judged by the ^{31}P resonance[16b] (Table 7, entry 5). Surprisingly, even at P/Rh = 2, 3, only the ^{31}P resonances of the mono(phosphine) complex and free **1** appeared, indicating the mono(phosphine) complex was
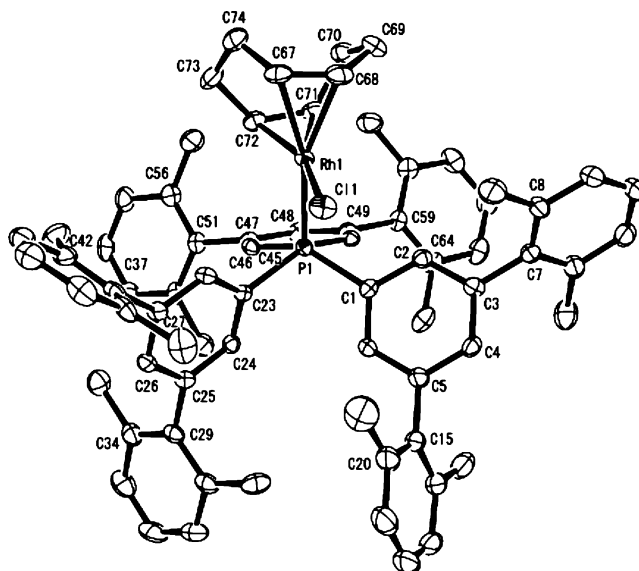

Figure 3. ORTEP drawing of [RhCl(COD)(**1**)] with thermal ellipsoids at the 50% probability level. Hydrogen atoms are omitted for clarity.

Table 8. Summary of Crystal Structure Data for the Complex RhCl(COD)(1)[a]

formula	C₇₆H₇₇Cl₇PRh
fw	1372.49
cryst syst	monoclinic
data collecn *T*, °C	−160
space group	*P*2₁/*c* (No. 14)
a, Å	16.4206(9)
b, Å	19.2472(9)
c, Å	22.0247(11)
β, deg	105.540(2)
V, Å³	6706.5(6)
Z	4
*d*calcd, g cm⁻³	1.359
cryst size, mm	0.27 × 0.17 × 0.07
habit	prismatic
μ, cm⁻¹	5.99
transmissn factors	0.9458−1.0000
no. of intensities (unique, *R*ᵢ)	66 233 (15 254, 0.053)
no. of intensities >3.00*σ*(*I*)	9936
no. of params	801
R[b]	0.067
*R*w[b]	0.096
GOF	0.836

[a] Conditions: radiation, graphite-monochromated, Mo Kα, λ = 0.710 70 Å; scan type *ω*−2*θ*; 2*θ*max = 55.0°. [b] *R* = Σ||*F*o| − |*F*c||/ Σ|*F*o|; *R*w = [Σ*w*(|*F*o| − |*F*c|)²/Σ*w**F*o²]^{1/2}, *w* = [0.0010*F*o² + 3.0000*σ*(*F*o²) + 0.5000]⁻¹.

obtained exclusively even in the presence of excess **1**. The mono(phosphine) complex RhCl(COD)(**1**) was isolated successfully from the solution, and single crystals suitable for X-ray analysis were obtained by slow diffusion of hexane into a CHCl₃ solution of the complex at room temperature. An X-ray crystallographic analysis was carried out, and the molecular structure of RhCl-(COD)(**1**) is shown in Figure 3. The crystallographic data and selected distances and angles are given in Tables 8 and 9, respectively. Figure 3 clearly indicates that the complex bears only one phosphine ligand (**1**) and the rhodium is settled in the bowl made by **1**. The isolated RhCl(COD)(**1**) showed the same ^{31}P resonance as observed in Scheme 2A (entry 5, Table 7). Furthermore, this isolated mono(phosphine) complex was active as the catalyst (5 mol %) in the hydrosilylation of cyclohexanone with HSiMe₂Ph at room temperature for 5 h to
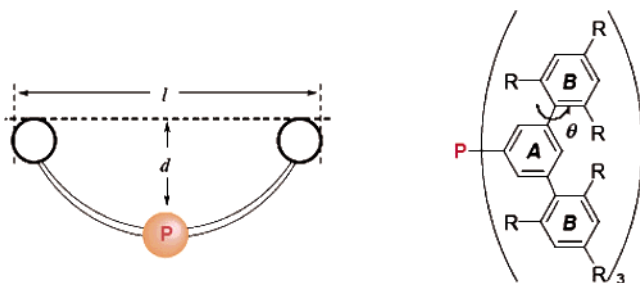
Figure 4. Diameters, depths, and dihedral angles of the bowl-shaped phosphines.

Table 9. Selected Bond Distances and Angles for RhCl(COD)(1)

Distances (Å)

P(1)−C(1)	1.824(6)	C(67)−C(68)	1.38(1)
P(1)−C(23)	1.817(6)	C(68)−C(69)	1.52(1)
P(1)−C(45)	1.837(6)	C(69)−C(70)	1.53(1)
P(1)−Rh(1)	2.285(1)	C(70)−C(71)	1.514(9)
Rh(1)−Cl(1)	2.365(2)	C(71)−C(72)	1.41(1)
Rh(1)−C(67)	2.208(7)	C(72)−C(73)	1.525(9)
Rh(1)−C(68)	2.229(6)	C(73)−C(74)	1.55(1)
Rh(1)−C(71)	2.115(7)	C(74)−C(67)	1.52(1)
Rh(1)−C(72)	2.131(7)		

Angles (deg)

Rh(1)−P(1)−C(1)	113.7(2)	P(1)−Rh(1)−C(67)	159.2(2)
Rh(1)−P(1)−C(23)	110.9(2)	P(1)−Rh(1)−C(68)	164.4(2)
Rh(1)−P(1)−C(45)	116.6(2)	P(1)−Rh(1)−C(71)	93.0(2)
P(1)−Rh(1)−Cl(1)	88.04(6)	P(1)−Rh(1)−C(72)	96.1(2)

Dihedral Angles (deg)

C(2)−C(3)−C(7)−C(8)	89.1(2)
C(4)−C(5)−C(15)−C(20)	78.0(2)
C(24)−C(25)−C(29)−C(34)	72.8(3)
C(26)−C(27)−C(37)−C(42)	66.4(3)
C(46)−C(47)−C(51)−C(56)	73.4(2)
C(48)−C(49)−C(59)−C(64)	81.7(2)

afford the product in 92% yield. In contrast, in the reaction of **4** with [RhCl(COD)]$_2$ at 60 °C (Scheme 2B), a considerable amount (23% and 47%, respectively, as a Rh complex) of the Wilkinson-type complex RhCl(**4**)$_3$ formed at P/Rh = 2, 3 in addition to the mono(phosphine) complex (Table 7, entry 6). Here, RhCl(**4**)$_3$ showed the same characteristic ^{31}P resonances (AB$_2$ system) as RhCl(PPh$_3$)$_3$[16c] (Table 7, entry 7), and the formation of RhCl(**4**)$_3$ was further confirmed by an FD mass spectrum, *m/z* 2294 (M$^+$).

Structural Difference between 1 and 4. The ^{31}P NMR study revealed that **1** favored the mono(phosphine) complexes, while **4** provided the bis- and/or tris(phosphine) species (Schemes 1 and 2). To explain this quite different coordination behavior, the optimized structures of **1** and **4** shown in Figure 2A,D were examined in detail. The diameters (*l* in Figure 4) of the bowls (1.99 nm for **1** and 1.95 nm for **4**) are similar. However, due to methyl substituents at the 2,2″,6,6″-positions of **1**, the dihedral angles (*θ*) between the phosphinated phenyl ring (ring A) and the phenyl ring in the meta positions (ring B) are quite different: 85.3 ± 0.5° for **1** and 44.7 ± 0.3° for **4**. Due to the large dihedral angles of **1**, a rim of the bowl comes up, and consequently **1** becomes a much deeper bowl than **4**: depths (*d* in Figure 4) of the bowls are 0.208 nm for **1** and 0.132 nm for **4**. The deeper bowl ligand would exclude the other identical deeper ligand on coordination (Schemes 1A and 2A), whereas two or three shallower bowls (**4**) can coordinate on the same metal (Schemes

1B and 2B). Even though the deeper bowl ligand keeps out the other identical deeper ligand, there is sufficient space for a catalytic reaction around the metal (catalyst) center of the resultant mono(phosphine) complex (Figure 3). This unique catalytic environment of the mono(phosphine) complex realizes the pronounced rate enhancement in the hydrosilylation reaction of ketones and ketimines (Tables 1 and 2). Conventional sterically bulky phosphine ligands such as P(*t*-Bu)$_3$ and PCy$_3$ are also known to generate low-coordinated (mainly bis) phosphine rhodium species[17] by steric congestion in the close proximity of the phosphorus atom of the phosphines. However, such steric hindrance near a catalytic center will obstruct coordination sites for coming substrate molecules. Consequently, overall catalytic activity with these ligands is lowered, as shown in Table 1.

In conclusion, the distinct rate enhancements of the hydrosilylation of ketones and ketimines are realized by utilizing BSP in the presence of a rhodium catalyst. The coordination of the deeper bowl phosphine is successfully regulated and the resultant mono(phosphine) species with a substantial space around the catalyst center would be responsible for the rate enhancement.

Experimental Section

General Considerations. All reactions were performed under an argon atmosphere using Schlenk techniques. Solvents were dried and purified prior to use by standard methods.[18] ^{1}H NMR (400.13 MHz), ^{13}C NMR (100.61 MHz), and ^{31}P NMR spectra (161.98 MHz) were recorded on a Bruker ARX 400 instrument. The ^{1}H NMR data are referenced relative to the residual protiated solvent (7.26 ppm) in CDCl$_3$. The ^{13}C NMR chemical shifts are reported relative to CDCl$_3$ (77.0 ppm). The ^{31}P NMR data are given relative to external 85% H$_3$PO$_4$. GC analysis was carried out using an Agilent GC 6850 equipped with an Agilent HP-1 column (length 30 m, 0.32 mm i.d.). TLC analyses were performed on Merck silica gel 60 F$_{254}$. Column chromatography was carried out with silica gel (Wako Wakogel C-200). FD mass spectra were recorded on a JEOL JMS-SX102A instrument at the GC-MS & NMR Laboratory of the Faculty of Agriculture, Hokkaido University. Elemental analysis was performed at the Center for Instrumental Analysis of Hokkaido University.

General Procedure for the Rhodium-Catalyzed Hydrosilylation. A typical reaction procedure in Tables 1−5 is as follows. Under an argon atmosphere, a phosphine ligand and a rhodium complex were placed in a 20 mL Schlenk flask. Anhydrous, degassed solvent was added by a syringe, and the mixture was stirred at room temperature for 2 h. Then, a substrate, tridecane (as an internal standard, 0.25 equiv with respect to the substrate), and a silane were added in this order by syringe. After the reaction, hydrolysis was performed by adding 1% HCl/MeOH and yields of the products were determined by GC analysis relative to the internal standard (tridecane).

Synthesis of the BSP. Although **1**[4,8] and **4**[10] have already appeared in the literature, a detailed preparation method and spectral data of **1** have not been reported. Therefore, those data of **1** are described as well as those of the novel phosphines **2** and **3**.

(17) (a) Yoshida, T.; Otsuka, S. *Inorg. Chim. Acta* **1978**, *29*, L257−L259. (b) Waal, D. J. A. D.; Robb, W. *Inorg. Chim. Acta* **1978**, *26*, 91−96. (c) Gusev, D. G.; Bakhmutov, V. I.; Grushin, V. V.; Vol'pin, M. E. *Inorg. Chim. Acta* **1990**, *175*, 19−21. (d) van Gaal, H. L. M.; van den Bekerom, F. L. A. *J. Organomet. Chem.* **1977**, *134*, 237−248.

(18) Armarego, W. L. F.; Perrin, D. D. *Purification of Laboratory Chemicals*, 4th ed.; Butterworth-Heinemann: Oxford, U.K., 1997.

Tris(2,2″,6,6″-tetramethyl-*m*-terphenyl-5′-yl)phosphine (1). To a solution of 5′-bromo-2,2″,6,6″-tetramethyl-*m*-terphenyl[19] (2.05 g, 5.61 mmol) in 33 mL of THF was added 3.53 mL (5.61 mmol) of *n*-butyllithium (1.59 M solution in *n*-hexane) dropwise over 15 min at −78 °C. The solution was stirred at that temperature for an additional 1 h, and phosphorus trichloride (0.257 g, 1.87 mmol) in toluene (5 mL) was added dropwise over 20 min to the cooled solution. The reaction mixture was further stirred at −78 °C for 1.5 h and at room temperature for 15 h. The solvent and all the volatiles were removed in vacuo, and then degassed toluene (32 mL) and water (8 mL) were added to the residue with vigorous stirring. The organic layer was separated and dried over anhydrous $MgSO_4$. The solution was filtered under an argon atmosphere, and volatiles were evaporated in vacuo to give crude products as a viscous material. The product, **1**, was obtained in 71% yield (1.18 g) as white microfine crystals by recrystallization from $CHCl_3$/MeOH (1/3). ^{1}H NMR ($CDCl_3$): δ 7.13 (dd, $^3J_{PH}$ = 7.5 Hz, $^4J_{HH}$ =1.4 Hz, 6H), 7.12−7.09 (m, 6H), 7.04−7.00 (m, 12H), 6.88 (t, $^4J_{HH}$ = 1.4 Hz, 3H), 1.87 (s, 36H). ^{13}C NMR ($CDCl_3$): δ 141.6 (d, $^3J_{CP}$ = 6.9 Hz), 141.1, 137.7 (d, $^1J_{CP}$ = 12.7 Hz), 135.6, 132.5, (d, $^2J_{CP}$ = 18.9 Hz), 130.1, 127.1, 127.0, 20.7. ^{31}P NMR ($CDCl_3$): δ −7.0. FD-MS: *m/z* 886 (M$^+$). Mp: 271.5−273.0 °C. Anal. Calcd for $C_{66}H_{63}P$: C, 89.35; H, 7.16. Found: C, 89.42; H, 7.40.

Tris(2,2″,4,4″,6,6″-hexamethyl-*m*-terphenyl-5′-yl)phosphine (2). In the same manner as **1**, the phosphine **2** was prepared from 5′-bromo-2,2″,4,4″,6,6″-hexamethyl-*m*-terphenyl[20] (2.20 g, 5.61 mmol). By recrystallization from $CHCl_3$/MeOH (1/6), **2** was afforded in 60% yield (1.09 g) as a white powder. ^{1}H NMR ($CDCl_3$): δ 7.13 (dd, $^3J_{PH}$ = 7.6 Hz, $^4J_{HH}$ = 1.5 Hz, 6H), 6.98−6.97 (m, 3H), 6.90 (s, 12H), 2.31 (s, 18H), 1.86 (s, 36H). ^{13}C NMR ($CDCl_3$): δ 141.4 (d, $^3J_{CP}$ = 6.9 Hz), 138.4, 137.5 (d, $^1J_{CP}$ = 12.3 Hz), 136.4, 135.5, 132.7 (d, $^2J_{CP}$ = 18.8 Hz), 130.6, 127.9, 21.0, 20.6. ^{31}P NMR ($CDCl_3$): δ −6.3. FD-MS: *m/z* 971 (M$^+$, 100%). Anal. Calcd for $C_{72}H_{75}P$: C, 89.03; H, 7.78. Found: C, 88.59; H, 7.67.

5′-Bromo-4,4″-di-*tert*-butyl-2,2″,6,6″-tetramethyl-*m*-terphenyl. This new compound was prepared from (4-*tert*-butyl-2,6-dimethylphenyl)magnesium bromide and 1-iodo-2,4,6-tribromobenzene in the same manner as the preparation of 5′-bromo-2,2″,4,4″,6,6″-hexamethyl-*m*-terphenyl.[20] ^{1}H NMR ($CDCl_3$): δ 7.36 (s, 2H), 7.17 (s, 4H), 6.98 (s, 1H), 2.15 (s, 12H), 1.40 (s, 18H). ^{13}C NMR ($CDCl_3$): δ 150.6, 143.8, 137.9, 135.7, 130.9, 129.7, 124.5, 122.8, 34.8, 31.9, 21.6. FD-MS: *m/z* 478 (M$^+$), 476 (M$^+$). Anal. Calcd for $C_{30}H_{37}Br$: C, 75.46; H, 7.81; Br, 16.73. Found: C, 75.09; H, 7.76; Br, 16.78.

Tris(4,4″-di-*tert*-butyl-2,2″,6,6″-tetramethyl-*m*-terphenyl-5′-yl)phosphine (3). The phosphine **3** was prepared from 5′-bromo-4,4″-di-*tert*-butyl-2,2″,6,6″-tetramethyl-*m*-terphenyl (700 mg, 1.46 mmol) in the same manner as **1**. By recrystallization (twice) from $CHCl_3$/toluene/MeOH (1/1/8), **3** was obtained in 50% yield (296 mg) as a white powder. ^{1}H NMR ($CDCl_3$): δ 7.10 (dd, $^3J_{PH}$ = 7.6 Hz, $^4J_{HH}$ = 1.5 Hz, 6H), 7.04 (s, 12H), 6.90−6.91 (m, 3H), 1.87 (s, 36H), 1.33 (s, 54H). ^{13}C NMR ($CDCl_3$): δ 141.8 (d, $^3J_{CP}$ = 6.9 Hz), 138.9, 137.9 (d, $^1J_{CP}$ = 12.5 Hz), 135.6, 133.2, (d, $^2J_{CP}$ = 18.7 Hz), 130.9, 124.5, 34.7, 31.8, 21.4. ^{31}P NMR ($CDCl_3$): δ − 6.6. FD-MS: *m/z* 1224 (M$^+$). HRMS (FD): *m/z* calcd for $C_{90}H_{111}P$ 1222.8423, found 1222.8430. Anal. Calcd for $C_{90}H_{111}P$: C, 88.33; H, 9.14. Found: C, 87.77; H, 9.32.

^{31}P NMR Study on a Mixture of $[RhCl(C_2H_4)_2]_2$ and the Phosphine (Scheme 1). In a NMR sample tube were placed $[RhCl(C_2H_4)_2]_2$ (3.9 mg, 0.01 mmol) and phosphine (0.02−0.06 mmol). The tube was evacuated and filled with argon, and degassed C_6D_6 (0.7 mL) was added under an argon flow to afford a homogeneous solution. The ^{31}P NMR spectrum was measured after 2 h at room temperature.

^{31}P NMR Study on a Mixture of $[RhCl(COD)]_2$ and the Phosphine (Scheme 2). In a NMR sample tube were placed $[RhCl(COD)]_2$ (4.9 mg, 0.01 mmol) and phosphine (0.02−0.06 mmol). The tube was evacuated and filled with argon, and degassed C_6D_6 (0.7 mL) was added. The tube was placed in an oil bath at 60 °C for 1 h, and the ^{31}P NMR spectrum was measured at room temperature.

Isolation of RhCl(COD)(1). To a 20 mL Schlenk flask charged with $[RhCl(COD)]_2$ (2.5 mg, 5 μmol) and ligand **1** (8.9 mg, 10 μmol) was added the degassed benzene (0.39 mL) under an argon atmosphere. After it was stirred for 1 h at 60 °C, the mixture was cooled to room temperature and concentrated in vacuo to give yellow solids. Single crystals of RhCl(COD)(**1**) suitable for X-ray structural analysis were obtained by slow diffusion of hexane into a $CHCl_3$ solution of RhCl(COD)(**1**). ^{31}P NMR (162 MHz, C_6D_6): δ 30.5 (d, $^1J_{P-Rh}$ = 153 Hz). FD-MS: *m/z* 1133 ([RhCl(COD)(**1**)]$^+$). Anal. Calcd for $C_{74}H_{75}ClPRh$: C, 78.40; H, 6.67; Cl, 3.27. Found: C, 78.34; H, 6.85; Cl, 3.14. The isolated complex was catalytically active. To a flask charged with the isolated RhCl(COD)(**1**) (11.3 mg, 0.01 mmol) was added degassed benzene (1 mL), and the solution was stirred for 10 min. Then, cyclohexanone (19.6 mg, 0.2 mmol) and dimethylphenylsilane (32.7 mg, 0.24 mmol) were added to the solution, and the reaction was carried out for 5 h at room temperature. Cyclohexanol was obtained in 92% (GC) yield after the desilylation with 2 M HCl/MeOH (2 mL).

X-ray Structure Determination of RhCl(COD)(1)·2CHCl$_3$. The data were collected with Mo Kα radiation ($λ$ = 0.710 70 Å) at −160 °C on a Rigaku Saturn CCD area detector to a maximum 2θ value of 55.0°. The structure was solved by direct methods using the program SIR92[22] and expanded using Fourier techniques. Non-hydrogen atoms, except for those of two disordered $CHCl_3$ molecules, were refined anisotropically. Hydrogen atoms were refined using the riding model. The final cycle of full-matrix least-squares refinement on F was based on 9936 observed reflections ($I > 3.0σ(I)$) and 801 variable parameters. A Sheldrick weighting scheme was used. Neutral atom scattering factors were taken from Cromer and Waber.[23] Anomalous dispersion effects were included in F_c.[24] All calculations were performed using the CrystalStructure crystallographic software package (version 3.6.0)[25]

Supporting Information Available: A figure giving the FD mass spectrum of $[RhCl(4)_2]_2$ and crystallographic data for RhCl(COD)(**1**) (as a CIF file). This material is available free of charge via the Internet at http://pubs.acs.org.

OM0503491

(19) Vinod, T. K.; Hart, H. *J. Org. Chem.* **1991**, *56*, 5630−5640.
(20) Ritleng, V.; Yandulov, D.; Weare, W. W.; Schrock, R. R.; Hock, A. S. Davis, W. M. *J. Am. Chem. Soc.* **2004**, *126*, 6150−6163.
(21) Tashiro, M.; Yamato, T. *J. Chem. Soc., Perkin Trans. 1* **1979**, 176−179.
(22) Altomare, A.; Cascarano, G.; Giacovazzo, C.; Guagliardi, A.; Burla, M.; Polidori, G.; Camalli, M. *J. Appl. Crystallogr.* **1994**, *27*, 435.
(23) Cromer, D. T.; Waber, J. T. In *International Tables for X-ray Crystallography*; Kynoch Press: Birmingham, U.K., 1974; Vol. IV.
(24) Ibers, J. A.; Hamilton, W. C. *Acta Crystallogr.* **1964**, *17*, 781.
(25) (a) Crystal Structure Analysis Package; Rigaku and Rigaku/MSC (2000−2004), 9009 New Trails Dr., The Woodlands, TX 77381. (b) Watkin, D. J.; Prout, C. K.; Carruthers, J. R.; Betteridge, P. W. Chemical Crystallography Laboratory, Oxford, U. K.